Switched battery DC–DC converters for low-power applications

Carlos Augusto Berlitz, Emeric Perez, Sami Oukassi, Bruno Allard, Gaël Pillonnet

Switched Battery DC-DC Converters for Low-Power Applications

Carlos Augusto Berlitz, *Student Member, IEEE,* Emeric Perez, *Student Member, IEEE,* Sami Oukassi, Bruno Allard, *Senior Member, IEEE* and Gaël Pillonnet, *Senior Member, IEEE*

***Abstract*—DC-DC conversion at an ultra-low operating frequency is one potential solution to maintain high efficiency in cases of ultra-low power delivery. Switched-capacitor converters (SCCs) have an inherent limitation to operate at low frequencies due to their charge-sharing losses. To overcome this issue, this paper explores a new DC-DC conversion family based on switched batteries. The so-called Switched-Battery Converter (SBC) is derived from the SCC by replacing the flying capacitors with batteries. The particular nature of the battery introduces constraints but offers degrees of freedom that redraw the trade-offs between switching frequency, charge-sharing losses, power density, and power efficiency. We demonstrate 97% power efficiency at 27 mW with only 100 Hz switching frequency using a button cell (69 mm^3) to achieve a 2:1 voltage conversion ratio. We also propose a 3:1 topology and various battery experiments to generalize the concept.**

***Index Terms*—DC-DC converter, battery, switched-capacitor, switching converter.**

I. Introduction

LOW-POWER electronic applications, especially wake-up and always-on circuits [1], [2], demand high efficiency and high power density DC-DC converters. Maintaining high power efficiency is challenging as the input power budget scales down. For example, achieving 90 % power efficiency at 1 µW means a loss power budget of 100 nW. All insignificant leakage and switching losses in sub-mW conversion become predominant at the µ-power scale.

A DC-DC converter operates around one or more central passive devices, traditionally capacitors and inductors, which are the strongest contributors to the converter's footprint. Switched capacitor converters (SCCs) are presented as the most popular solution for integration to reach high power density in low-power applications [3], [4]. The output impedance of SCCs scales inversely with the operating frequency and the values of the flying capacitors [5], [6]. The power efficiency is directly impacted by the switching losses increasing with the operating frequency. If we try to maintain high efficiency at low input power by limiting the operating frequency, we end up impacting the converter footprint. New technologies of high-density integrated capacitors do not significantly improve the SCC power density or efficiency due to the inherent limitation related to the charge-sharing losses.

We proposed the usage of batteries as an alternative passive device to address the fundamental limits of SCCs at low power scale [7]. Batteries present a few decades higher energy storage capability when compared to traditional devices, as shown in Table I, at the expense of low power capability mainly linked to much higher equivalent series resistance (ESR). However, this limitation does not come into play when operating at low switching frequency. Based on the SCC structure, we propose a novel topology called the Switched Battery Converter (SBC), shown in Fig. 1, which replaces traditional technology passive devices by batteries.

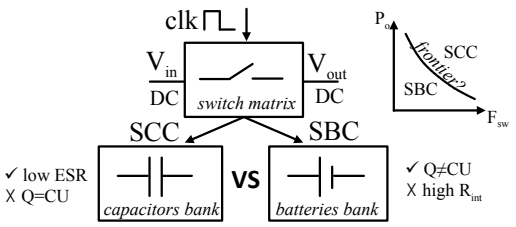

Fig. 1. Switched DC-DC converter using battery as passive device

The proposed topology effectively addresses the limitations associated with lower switching frequencies in switched capacitor converters (SCCs) and introduces new trade-offs between loss mechanisms and frequency by significantly reducing the charge-sharing loss component. In SCCs, power losses can be classified into three main categories based on their relationship with the switching frequency of the converter. The first category is switching loss, which increases proportionally with the frequency. The second category is conduction loss, which decreases inversely with the frequency due to the presence of charge-sharing loss. The third category is constant leakage loss. The optimal frequency for minimizing power loss occurs when the switching loss and conduction loss are balanced, thereby restricting the available sizing choices for SCCs. In the proposed switched battery converter (SBC), the switching loss is nearly eliminated at the expense of additional conduction loss, resulting in competitive ultra-low-power, ultra-low-switching frequency DC-DC converters.

This work distinguishes itself from battery power management units, which often involve battery switching to create resilient battery packs and PV-battery interfaces for voltage balancing [8] [9]. Battery management systems (BMS) [10] [11] featuring dynamic reconfiguration have been introduced as an emerging field aimed at overcoming performance limitations imposed by the weakest cells in battery systems, resulting in underutilized sections. These configurable battery systems offer several advantages, including fault tolerance, extended energy delivery, charge and temperature balancing, and customized terminal voltages, while coordinating batteries

Manuscript received April 19, 2021; revised August 16, 2021.

TABLE I
OFF-THE-SHELF DEVICES SAMPLE WITH MM^3 VOLUME

Passive	Metric	Energy density $[J.mm^{-3}]$	Power density $[W.mm^{-3}]$	Power density $[\mu W.mm^{-3}]$	Voltage/current rating	ESR $[\Omega]$	Surface $[mm^2]$	Volume $[mm^3]$
	Frequency	-	@ SRF/10	@ 1 Hz				
Battery (V6HR)		$\mathbf{3.6\times10^{-1}}$	N.A	**345**	0.018 A	6	35.2	74
Capacitor [12]		33×10^{-6}	**2**	33	6.3 Vdc	15×10^{-3}	31.4	60
Inductor [13]		70×10^{-9}	0.01	0.07	0.145 A	2.9	16	69

of different ages and chemistries. In our proposed system, batteries are used as intermediate storage elements, meaning that each battery does not change its state of charge (SoC) after one switching period during the DC-DC operation. In other words, only a small fraction of the battery's energy capability is utilized during the period, serving as an intermediate energy reservoir. To the best of the authors' knowledge, the utilization of batteries in this specific context has not yet been covered in the literature.

A first SBC demonstration was described in our previous paper [7]. This article introduces a detailed comparison with SCC in a 2:1 configuration in section III, analysis of battery behavior (self-biasing, state of charge, lifetime), and the impact of different chemistries in section IV. In section V, we also introduce multiple-battery SBCs to generalize the approach.

II. BATTERY AS A FLYING PASSIVE DEVICE

The conversion of electrostatic and electromagnetic energies into electrical energy is faster than the chemical one, making batteries have higher electrical time constants and a slower dynamic response. Batteries, as a flying device inside a DC-DC converter, introduce a limitation in switching frequency. In an SCC, this is favorable in terms of losses but not output voltage ripple. However, having a high time constant constitutes a kind of electrical energy inertia, which also contributes to reducing the voltage ripple across the batteries' terminals and the output voltage.

Batteries excel in energy density when compared to traditional passives of similar dimensions, as shown in Table I. Due to the first-order correlation between power density and operating frequency for capacitors and inductors, as shown in Figure 2, it can be observed that batteries outperform traditional flying passive components in terms of power density, even when their equivalent series resistance (ESR) is three times higher than that of capacitors. Therefore, the focus of this paper is on low output current DC-DC converters (<10mA), where conduction losses are not the primary concern for maintaining decent power efficiency. As highlighted in previous studies [14] [15], very low-power DC-DC converters require ultra-low switching frequencies to maintain low switching losses, which result in larger components to achieve low output ripples. In some cases, the required component size is comparable to that of converters with much higher power delivery capabilities. This paper aims to address the question of the potential power range where the switched battery converter (SBC) could serve as a credible alternative to switched capacitor converters (SCC).

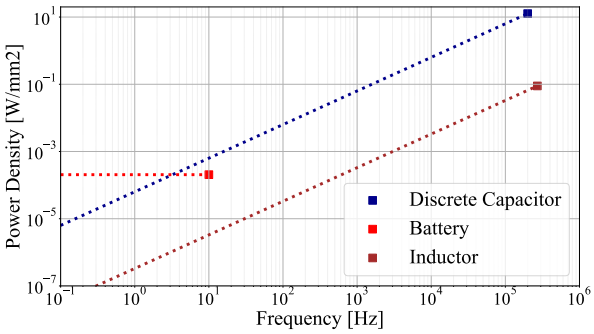

Fig. 2. Battery power density advantage at low operating frequency

Miniaturization of solid-state batteries is improving, and the energy density offers high value even at the mm^3 scale [16], [17]. Liquid electrolyte batteries require a larger packaging solution but are capable of higher output power. Solid-state thin film batteries (TFBs) with a total thickness down to 100 µm [16] can be integrated directly onto silicon substrates, presenting much higher energy and power density. This opens up the possibility of small packaging battery management systems such as [18].

III. SWITCHED-BATTERY CONVERTERS

The proposed switched-*battery* converter (SBC) incorporates at least one battery as the central flying passive component. This introduces a new set of challenges for defining a DC-DC converter state sequence. First, the need to keep the battery within its regular voltage operating limits poses the challenge of finding a set of phases in which the arrangement of components maintains the output voltage at the desired level. Second, there is a need for sequencing the phases to maintain charge balance throughout the converter cycle.

During the SBC steady-state operation, the battery is subject to at least one charging and one discharging phase. During these phases, the charge flowing through the battery should be smaller (<<1%) than the battery's overall rated capacity. Due to this very small depth of discharge (DoD) operation, the battery works in a µ-cycle manner, as introduced in [7]. This µ-cycle operation ensures that the DoD does not affect the battery's average voltage while expanding the battery's cycle life dramatically [19].

A. Sequence of States

The proposed SBC uses different topology phases (a fixed state of connections between the devices) sequenced in a

particular way, forming a cycle. This cycle repeats during steady state operation.

As is the case with SCC, different cycles allow for different voltage conversion ratios. For a working cycle to be convenient in the SBC, it has to fulfill the following criteria: i) the average voltage across each battery has to remain fixed around their operational voltage (dictated by the battery's electrochemical reaction), ii) the energy given/received by each battery has to achieve balance during one cycle, iii) the voltage created by a battery network arrangement and the input source has to be equal to the output voltage in all phases.

The study here is limited to cycles using phases of equal time duration. This restriction aims at reducing the scope but is not related to any SBC topology limitation.

B. Power Efficiency Analysis

Differently from the SCC, the SBC does not present intrinsic charge sharing losses. Apart from the static losses due to the control of the switches, the oscillator and overall quiescent consumption, the losses in a SBC are dominated by the conduction losses. We can model the SBC assuming an ideal DC voltage conversion ratio under no load condition, represented by an ideal transformer and all conversion losses caused by an output impedance R_{out} creating an output voltage drop [20].

Despite similarities in topology between the SCC and SBC, both systems present different loss mechanisms. However, due to the well established SCC formalism and model, we start the analysis of the SBC dynamic losses analyzing the SCC approach. As presented in [20], SCC converters operate in either one of two operating conditions, or between them. One of the drawbacks mentioned refers to low switching frequencies, where losses and output impedance are primarily determined by the limited charge storage capability of capacitors, leading to what is known as the slow switching limit (SSL) [21]. In this regime, the output impedance is observed to be inversely proportional to the switching frequency for SCC. However, in the case of batteries, the relationship between transferred charge and voltage is not linear. As a result, the voltage drop across the batteries during operation remains nearly independent of the switching frequency. This implies that the output impedance does not increase significantly with low-frequency operation. The other operating regime is referred to as the fast switching limit (FSL), which occurs at high operating frequencies in SCC. In this regime, the output impedance and losses are primarily influenced by the on-state resistances of the switches and the equivalent series resistance (ESR) of passive devices.

The frequency of the inflection point between FSL and SSL (f_{lim}) is given by [20] as the inverse of the product between the switch on-state resistance and the capacitance of the flying capacitor. The circuit is operating in FSL if the operating frequency is greater than f_{lim}, and in SSL otherwise. As the SBC uses a battery as the flying passive, we consider the equivalent capacitance to be infinite (f_{lim} is equal to 0) and the circuit is thus always operating in FSL. As the output impedance is frequency independent, the SBC losses are dominated by the conduction losses, and it is natural to start the analysis of SBC losses by the FSL equivalent resistance derived from [20] given by:

$$R_{FSL} = \sum_i \frac{R_i (a_{r,i})^2}{D_i} \tag{1}$$

Where R_i is the on-resistance of the i^{th} switch, D_i is the duty cycle of the i^{th} switch, and $a_{r,i}$ is the normalized charge flow through each switch during the phase in which the i^{th} switch is on. The values for $a_{r,i}$ are determined by circuit inspection and normalized by the total output charge, q_{out}, similarly to [20].

However, the SCC's R_{FSL} does not take into account the flying passive series resistance, as capacitor ESRs are generally negligible against the on-resistance of the switches. Batteries, on the other hand, have more internal impedance than the ESR of any common flying capacitor, which can impact the overall equivalent series resistance of the converter meaningfully. Adding the internal resistance of the battery to (1) gives the equivalent output resistance of the SBC converter to be defined as:

$$R_{out} = \sum_i \frac{R_i (a_{r,i})^2}{D_i} + \sum_j \frac{R_{int,j} (a_{b,j})^2}{D_j} \tag{2}$$

Where $R_{int,j}$ is the internal resistance of the j^{th} battery, D_j is the duty cycle in which the j^{th} battery is utilized and $a_{b,j}$ is the normalized charge flow through the battery while it is being used. Circuit inspection is used to obtain the value of $a_{b,j}$ and later is normalized by the total output charge, q_{out} similarly to $a_{r,i}$. This result allows to estimate SBC's conversion losses using only structural parameters.

IV. Performance comparison: SCC vs SBC

The purpose of this comparison is to assess the performance of SCC (Switched Capacitor Converter) against SBC (Switched Battery Converter) specifically at ultra-low switching frequency, in the Hz range. The motivation behind this investigation is rooted in previous findings that highlight the need for high efficiency in low-power delivery scenarios, which can be achieved by operating at extremely low switching frequency to minimize switching losses. In this context, conduction loss is not the dominant factor, which provides an opportunity for SBC to excel despite the battery's ESR (Equivalent Series Resistance) being several orders of magnitude higher than the one of capacitors. However, it is worth noting that the operating frequency range is suitable for SCC, as charge sharing loss increases inversely proportional to the frequency. To maintain a competitive edge for SCC, we have opted to use the same component size, enabling the utilization of larger flying capacitors to partially compensate for the reduction in switching frequency.

The proposed SBC is compared to a SCC using the same power stage circuit (Fig. 3a) at the same output power levels and operating frequencies. The capacitor and battery-under-test (BUT) have similar dimensions. The SBC circuit is shown in Fig. 3b. The circuit is implemented using a

commercial switched-capacitor voltage converter integrated circuit (LM2663).

The circuit uses a 2:1 topology operating in two phases. In phase ϕ_1, the input voltage source V_{in} provides charges (Q_{ϕ_1}) to the flying passive device (respectively, the battery for the SBC configuration and the capacitor for the SCC one). In phase ϕ_2, the flying passive device is directly connected to the output, providing charge Q_{ϕ_2}. Under normal operation output node of the SCC is connected to a large output capacitor while SBC output node is directly connected to the load.

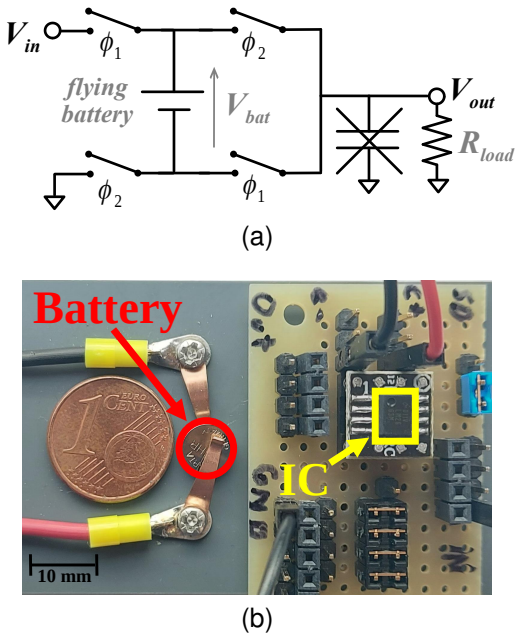

Fig. 3. (a) 2:1 converter power stage electrical schematic and (b) implementation of 2:1 SBC using LM2663 and V6HR

The off-the-shelf IC LM2663 includes an oscillator whose frequency can be adjusted externally using a network of capacitors. The IC has a footprint of 19 mm^2, which is similar to the BUT and flying capacitor used in the experiment and are of equivalent dimensions as presented in Table I. The V6HR BUT used in the experiment is a NiMH device, which is considered to be a safer technology than others, as Li-Ion. Moreover, the NiMH technology also offers an open circuit voltage level of 1.2 V $\pm 10\%$) which is suitable for the implemented 2:1 topology that converts 2.6 V (V_{in}) into 1.3 V (V_{out}).

Using equation (2), the SBC's equivalent output resistance is calculated to be 6.4 Ω. As explained in Section III-B, this value is largely independent of the switching frequency but is strongly influenced by the internal battery contribution, which accounts for approximately 90% of the total equivalent output resistance. The converters are compared over a range of operating frequencies spanning three orders of magnitude (100 Hz, 1 kHz, and 10 kHz) and with an output current ranging from 100 µA to 30 mA. These current values represent 1/6 C up to 5 C of the BUT, which are within its regular operating limits.

A. Steady-State Operation

A typical operation curve of the SBC configuration (without output capacitance) in steady-state 2:1 is shown in Fig. 4a, where appears a similar behavior of the output voltage V_{out} is observed during ϕ_1 and ϕ_2, with a small difference in average value. During ϕ_1, V_{out} is the result of the difference between the input voltage V_{in} and the battery voltage V_{bat}, while during ϕ_2 the battery is connected directly to the output. V_{bat} exhibits a different behavior in both phases (Fig. 4b). It highlights the two kinds of the ripple present in V_{bat}, as introduced in [7]: an ohmic drop and a redox drop. The former is an almost instantaneous ohmic IR drop V_{IR} due to the BUT internal resistance, and the latter is the redox voltage V_{redox} caused by the redox reactions due to the µ-cycling [7].

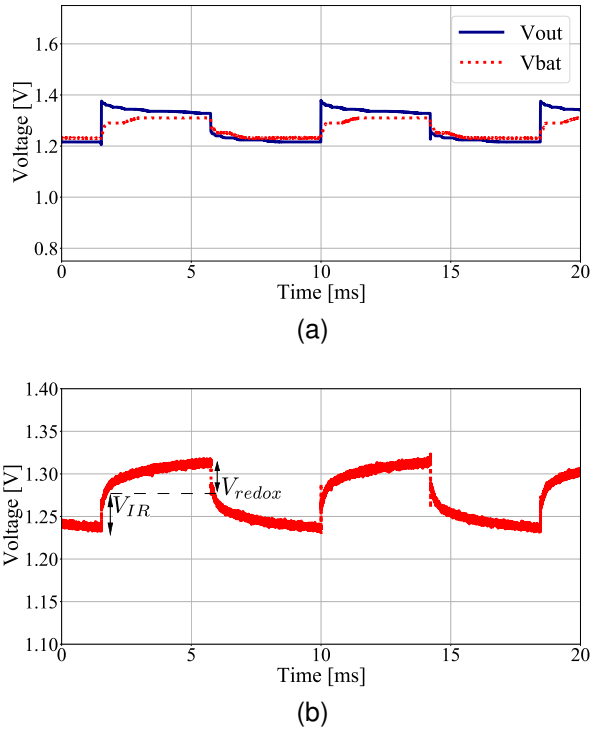

Fig. 4. Experimental steady state operation of a 2:1 SBC at 100 Hz: (a) output and battery voltages and (b) battery voltage ripple

B. Relative Output Voltage Ripple

A large output voltage ripple is unacceptable in most applications [22], making it a key performance benchmark in DC-DC converters. For SCCs of a given passive size, the output voltage ripple is highly degraded by a low operating frequency. Since the SBC operates at low and ultra-low frequencies, it is of high importance that it maintains an acceptable output voltage ripple.

Fig. 5 shows the relative output voltage ripple versus the output current at 0.1 and 10 kHz for the SBC and SCC, respectively. The SBC topology, which operates without any output capacitance, exhibits an output voltage ripple of less than 5% even at a frequency of 100 Hz while delivering 20mA to the load. On the other hand, the SCC, lacking an

output capacitor, experiences an output voltage ripple reaching over 30% under similar conditions. To reduce the ripple to a comparable level, a bulky 5.0F output capacitor has been added to the SCC leading to the results shown in Figure. 5.

Without output capacitor, the SBC presents moderate output voltage ripple at low operating frequency, thus reducing the switching loss. Ripple in the SCC is caused by the capacitor's fundamental principle of having the voltage between the terminals of the device directly dependent on the amount of its stored charge ($Q = CV$). For the SBC, as explained in Section I, the voltage between the battery's terminals is not directly dependent on the quantity of transferred charge. The lower ripple of the SBC then comes from the battery presenting a higher electric inertia compared to a capacitor. The slow change in the battery voltage is related to the V_{redox} effect seen in Fig. 4b, related to the redox chemical reaction inside the battery.

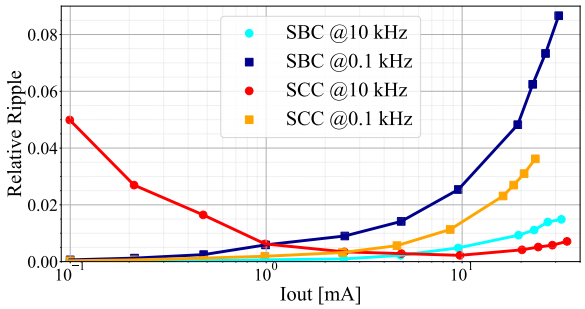

Fig. 5. Comparison of relative output voltage ripple between 2:1 SBC and 2:1 SCC

C. Power Efficiency

As the whole circuit is powered by V_{in}, the input power includes the control of the switches, the oscillator and overall quiescent consumption of the off-the-shelf IC.

The efficiency of the SBC is presented at three different frequencies and different current amplitudes in Fig. 6a. As detailed in III-B, the conduction losses and thus overall efficiency of the SBC is highly independent of the switching frequency. A small difference is seen for low output currents due to the quiescent current of the active circuit itself (from 30 to 50 µA). Fig. 6b gives the performance at 100 Hz for the SCC (which uses a large output decoupling capacitor) against the SBC (with no output capacitor).A focus around the 2.5 mA operating point is provided for different switching frequencies. Peak efficiency is reached at the lowest switching frequency (e.g. 0.1 kHz) for SBC but at the highest switching frequency (e.g. 10 kHz) for SCC.

The SBC presents better efficiency than the SCC at low operating frequency as the SSL losses of the SCC (such as charge sharing losses) are noticeable, decreasing the SCC efficiency. As explained in Section III-B, the SBC does not feature an SSL regime. Besides the SBC's efficiency is strongly impacted by the internal resistance of the battery (which is higher than the SCC's capacitor ESR). This higher resistive component is still less important than the SSL component of the SCC at low frequency.

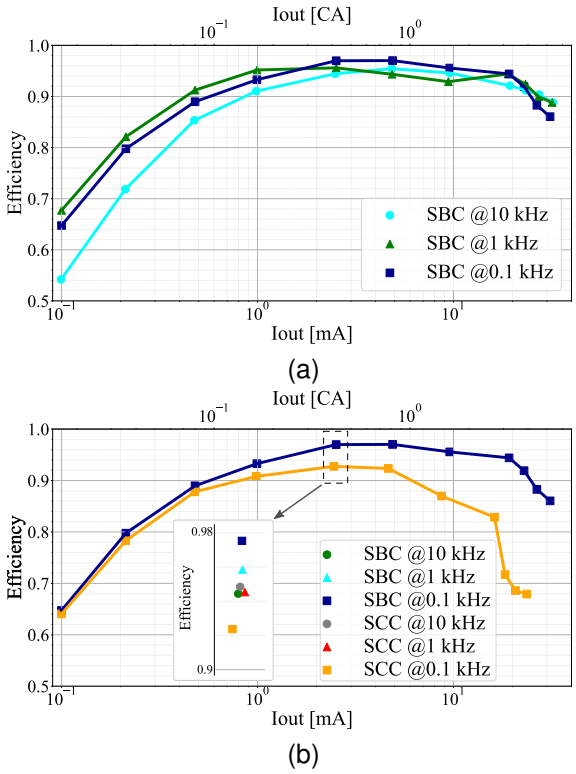

Fig. 6. Efficiency of the 2:1 SBC: (a) independence of frequency and (b) advantage against SCC at 100 Hz

The efficiency gain in favor of the SBC at low output current is higher for moderate and low frequencies when operating without output capacitance. The SCC equivalent output resistance at high frequency is dominated by the FSL effects, matching the analysis detailed in Section III-B presenting similar losses and performance as the SBC.

The battery configuration manages to hold a high efficiency (>90%) for a respectable output current range (up to 20 mA). The SBC's maximum output power maintaining such high efficiency is approximately 27 mW at 100 Hz, and 32 mW at 1 kHz and 10 kHz. A rule of thumb gives an estimate of the power volume density of 364 µW/mm^3 at 100 Hz and 432 µW/mm^3 at 1 kHz and 10 kHz (referred solely to the battery's volume).

D. Battery Voltage Self-Adjustment

The battery self-adjusts its voltage to achieve charge balance, similar to how capacitors do in SCC, by changing its voltage towards the steady-state operation voltage value imposed by the topology during SBC operation, such as in the 2:1 configuration where $V_{bat} = V_{in}/2$), in a kind of Battery Voltage Self-Adjustment (BVSA). This behavior poses no risk to battery life, provided that the voltage remains within the battery's voltage limits for charge and discharge.

To further clarify, the BVSA process causes the battery voltage to converge towards the steady state value imposed by the SBC topology, which ensure that the average output voltage remains constant. However, during the convergence

time, the battery voltage, and thus the output voltage, may experience some ripple. This ripple reduces as the BVSA process progresses and eventually reaches a minimum point. The BVSA mechanism reveals that the battery functions as a steady voltage provider within short-term, while adopting the characteristics of an adjustable voltage source (resembling a capacitor) over extended periods.

The efficiency during the power-on dynamic may be affected by the BVSA process depending on the initial voltage of the battery. If the battery's initial voltage is higher than the required steady state value, the efficiency will start at a high value and gradually decrease until it reaches a steady state value. On the other hand, if the battery's initial voltage is lower than the required for steady state value, the efficiency will start at a lower value and gradually increase until it reaches a steady state value.

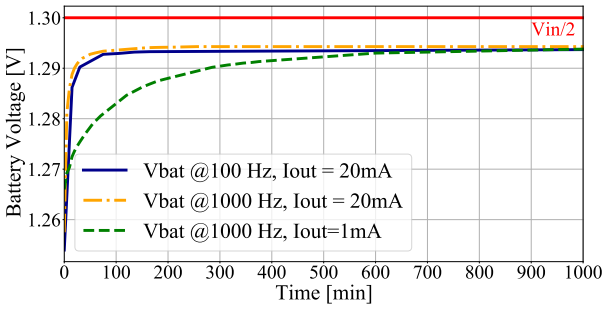

Fig. 7. Impact of frequency and current on the battery voltage evolution during power-on dynamic in the 2:1 SBC

The large electric inertia of batteries results in longer settling times to reach a steady-state voltage. The settling time is independent of the operating frequency in the 2:1 topology, as observed experimentally. However, the output current does have an impact on the output voltage transient during power-on dynamic, as shown in Fig. 7. For an output current of 20 mA, it takes more than 85 minutes (500 thousand cycles) to reach a steady-state voltage at 100 Hz, and about half this time at 1000 Hz, which is 10 times higher frequency. In both cases, the battery starts with a similar voltage (1.254 V at 100 Hz and 1.257 V at 1000 Hz). At the same frequency (1000 Hz), the current and the transferred charge are preponderant factors in the output voltage evolution. For example, at 20 mA, it takes around 5 minutes for a 24 mV increase in battery voltage, whereas it takes 50 minutes for a gain of 13 mV at 1 mA. In both cases, we are in the exponential part of the voltage increase.

E. Charge Balance and Lifetime

Battery charge balance is a crucial aspect of the SBC operation, as the battery must receive the same amount of charge that it supplies to the load. However, achieving perfect charge balance over each complete cycle is not always possible, especially in symmetrical cycles (where each phase has the same duration). Despite this, experimental data has shown that small imbalances over duty cycles are still able to achieve steady-state operation. This is due to the self-balancing behavior of the battery, which adjusts its voltage to reach the required charge balance. In steady state operation, the voltage of the flying batteries changes towards the steady state operation voltage value imposed by the topology. This behavior presents no risk to battery life as long as the value is still inside the battery's voltage limits for charge and discharge.

One of the primary concerns regarding the utilization of batteries in DC-DC converters is their limited lifetime, typically spanning from 10^3 to 10^4 fully charge/discharge cycles. However, the battery employed in the SBC configuration experiences a significantly higher number of cycles due to the Hz range of operation. Even at a conservative frequency of 1 Hz, a 10-year operation would necessitate supporting nearly one billion cycles. Nevertheless, the battery in SBC introduces a unique scenario compared to conventional battery usage: it operates with an extremely low depth of charge, approximately 1 ppm. This characteristic fundamentally changes the perspective when evaluating its lifetime within this particular context. To address this concern, we conducted a comprehensive long-term experiment over several weeks at 1 kHz, subjecting the battery to over one billion micro-cycles. Following the experiment, we evaluated the battery's performance by analyzing the Q(V) curve and observed no significant degradation. This finding suggests that the impact of SBC operation on battery performance differs significantly from regular battery usage, which involves almost fully charge/discharge cycles. Moreover, as mentioned in Section IV-D, the capacitive component of the battery's charge transfer mechanism plays a role in extending its lifetime by reducing electrochemical stress. Consequently, the battery in SBC operates not only in battery mode but also in capacitive mode, effectively mitigating its electrochemical degradation. Additionally, the relatively low current levels used in the SBC (compared to typical battery usage) may also help to reduce degradation over time [23]. However, it is important to note that battery degradation can be a complex and multifactorial phenomenon, and further research may be needed to fully understand the long-term impact of SBC operation on battery performance.

F. Battery's Chemistry Impact on SBC

A limitation of the 2:1 configuration is that the output voltage (V_{out}) needs to be at the same voltage range as the battery voltage (V_{bat}). Despite the battery's self-adjustment mechanism detailed in Section IV-D, this behavior remains very limiting, as the battery's operating voltage limits are quite restrictive. To explore other output voltage values, one solution is to use different battery chemistry, such as Li-Ion, for example. Such battery chemistry can also have other advantages and disadvantages when used in a SBC.

To experiment with a Li-ion battery (TS621E) with similar dimensions to the previous NiMH device, the same setup and voltage ranges were used, despite the Li-ion having a larger voltage range capability (1.5 V). The Li-ion has a lower nominal capacity (2.5 mAh compared to 6 mAh) but still managed to maintain high efficiency (>90%) for an output current range of 2 mA at frequencies of 100 Hz and 1 kHz.

With such high efficiency, the 2:1 SBC using a Li-ion battery has a peak output power of 2.57 mW at 100 Hz and 2.74 mW at 1 kHz, representing a power volumetric density at 100 Hz of 34.7 μW/mm^3 (referring solely to the battery's volume). A peak efficiency of 97% is achieved despite the lower power density. The battery's nominal capacity is not expected to affect the power output at first order, and at second order the reduction in the nominal battery capacity creates an increase in the internal resistance.

Another explored battery chemistry is a solid-state battery having a $LiCoO_2$ cathode, LiPON ceramic electrolyte, and a lithium anode. The thin film battery is implemented using the same 2:1 SBC circuit but converts 7.6 V into 3.8 V. The EFL700 thin film battery (STMicroelectronics) has a larger internal resistance (around 10 times that of the NiMH) and a limited nominal capacity of 1 mAh. The peak efficiency is 78% at 1 kHz and 76.8% at 100 Hz for 2 mA output current. Keeping an efficiency of 70%, it manages an output power of roughly 24 mW at both frequencies, reinforcing the frequency independence. Such power represents a power volumetric density of 200 μW/mm^3. The higher density can be attributed to the thin film battery's form factor (low thickness with a larger surface) and higher operating voltage.

The results show that different battery chemistry still present acceptable performances to the 2:1 SBC, as long as they are kept operating with a very small depth of charge, even for batteries with low capacity. However, lower capacity linked with a higher internal resistance has an impact on a smaller output current range when operating at high efficiency. The higher voltage operating range benefits when exploring higher output power to some degree, as the capacity and internal resistance still limit the achievable output current. Some batteries also present a wider voltage range, favoring the exploration of flexible operating conditions. Nevertheless, as the tested batteries also presented the self-adjustment behavior described in Section IV-D, it is clear that they successfully enable a wider operating voltage range for the 2:1 SBC.

V. Switched Multiple-Batteries Converters

Despite the wider operating voltage range enabled by different battery chemistries, it remains somewhat restrictive as the magnitudes of the batteries' voltages do not vary significantly. Additionally, the output voltage continues to have a strong correlation with V_{bat}, as previously illustrated. In an effort to mitigate these limitations, we have investigated the use of multiple batteries in the SBC configuration, which opens up the possibility of operating with multiple phases. It is not necessary for each battery to be identical or have the same voltage. The exploration of multiple switched batteries also aims to expand the range of available voltage ratios for the converter.

A. Systematic Topology Exploration

To identify operational cycles utilizing multiple switched batteries, we must still adhere to the limitations outlined in Section III-A. In addition to these individual phase restrictions, we must also fulfill the following conditions:

$$V_{out,j} = a_{0,j} \cdot V_{in} + \sum_i a_{i,j} \cdot V_{bat,i,j} \tag{3}$$

Here, $V_{out,j}$ represents the output voltage of the j^{th} phase, $V_{bat,i,j}$ denotes the battery voltage of the i^{th} battery during the j^{th} phase, and $a_{i,j} = -1/0/+1$ signifies the i^{th} element during the j^{th} phase (where element 0 corresponds to the voltage source). The value of $a_{i,j}$ indicates whether the element (either the voltage source or one of the batteries) is disconnected (0), connected in series to the load in a positive orientation (1), or in a negative orientation (-1). In this context, a positive orientation implies that the element adds voltage relative to the ground, leading to a higher V_{out}, while a negative orientation subtracts voltage towards a lower V_{out}. Additionally, we impose the condition that for each phase, at least one of the batteries must be connected to the load.

In order to identify suitable SBC cycles using multiple batteries, we conduct a semi-exhaustive search. To simplify the algorithm and reduce computation time, we restrict the search to the use of two groups of batteries ($V_{bat,1}$ and $V_{bat,2}$). Figure 8 illustrates the possible conversion ratios V_{in}/V_{out} for multiple-battery SBC, plotted against the $V_{bat,i}/V_{out}$ ratio. The value of $V_{bat,i}$ corresponds to the value of $V_{bat,1}$ and/or $V_{bat,2}$, as some cycles utilize both batteries at the same voltage level. For example, choosing $V_{in}/V_{out} = 3$ (a 3:1 SBC) offers numerous options for $V_{bat,i}/V_{out}$. However, not all combinations of $V_{bat,1}$ and/or $V_{bat,2}$ can yield a functional cycle. For instance, there may be a working cycle with one group at $4 \cdot V_{out}$ and the other at $1 \cdot V_{out}$, but not with $4 \cdot V_{out}$ and $2 \cdot V_{out}$.

The highlighted configuration in Fig. 8, which corresponds to a 3:1 SBC, has been experimentally validated. This configuration utilizes $V_{bat,1}$ and $V_{bat,2}$ at the same voltage level of $2 \cdot V_{out}$, resulting in $V_{bat,i}/V_{out}$ of 2 for both batteries. The implemented configuration involves both groups, with a single flying battery each (B1 and B2), operating in three phases as depicted in Fig. 9b. During phases ϕ_1 and ϕ_2, V_{in} supplies charges (Q_{ϕ_1} and Q_{ϕ_2}) to batteries B1 and B2, respectively. In phase ϕ_3, both batteries release charge Q_{ϕ_3} to the circuit. Since the durations of all three phases are equal ($t_{\phi_1} = t_{\phi_2} = t_{\phi_3}$) and I_{out} remains constant throughout the cycle, it follows that $Q_{\phi_1} = Q_{\phi_2} = Q_{\phi_3}$. By exchanging equal charges over the three phases, B1 and B2 maintain charge balance throughout the cycle.

Fig. 9b illustrates that during phase ϕ_3, the voltage source is connected in the opposite polarity to V_{out}, resulting in energy being received from the circuit. This behavior is unconventional in typical DC-DC converters, where the voltage source usually only provides energy to the circuit. However, in the case of the 3:1 SBC configuration, this unorthodox behavior is necessary to achieve charge balance and to reduce the strong dependence between V_{bat} and V_{out}.

Fig. 9a depicts the power stage circuit of the 3:1 SBC topology. The switches in the circuit carry a current of either I_{out} or 0, depending on the phase. With the exception of $S_{i,a}$ and $S_{1,a}$, each switch conducts current only during one phase. Table II presents the voltage values across the switch

TABLE II
VOLTAGE ACROSS SWITCHES AND BATTERY CHARGE MOVEMENT IN EACH PHASE OF 3:1 SBC

Phase	Voltage across terminals								Charge	
	$S_{1,a}$	$S_{1,b}$	$S_{1,c}$	$S_{2,a}$	$S_{2,b}$	$S_{2,c}$	$S_{i,a}$	$S_{i,b}$	B1	B2
ϕ_1	0	0	Z	Z	Z	Z	0	$V_{in}/3$	$+Q$	0
ϕ_2	Z	Z	Z	0	0	$V_{in}/3$	0	$V_{in}/3$	0	$+Q$
ϕ_3	0	$V_{in}/3$	0	0	$V_{in}/3$	0	$V_{in}/3$	0	$-Q$	$-Q$

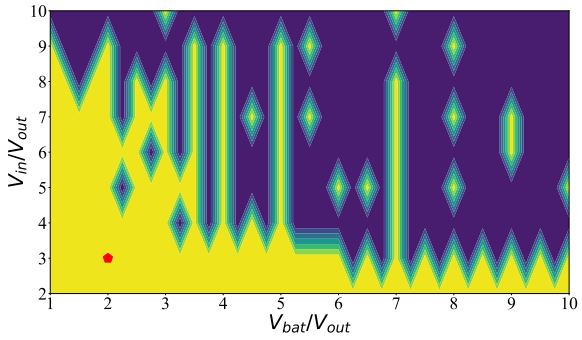

Fig. 8. SBC conversion ratios depending on V_{bat}/V_{out}. Yellow dots denote a possible conversion ratio.

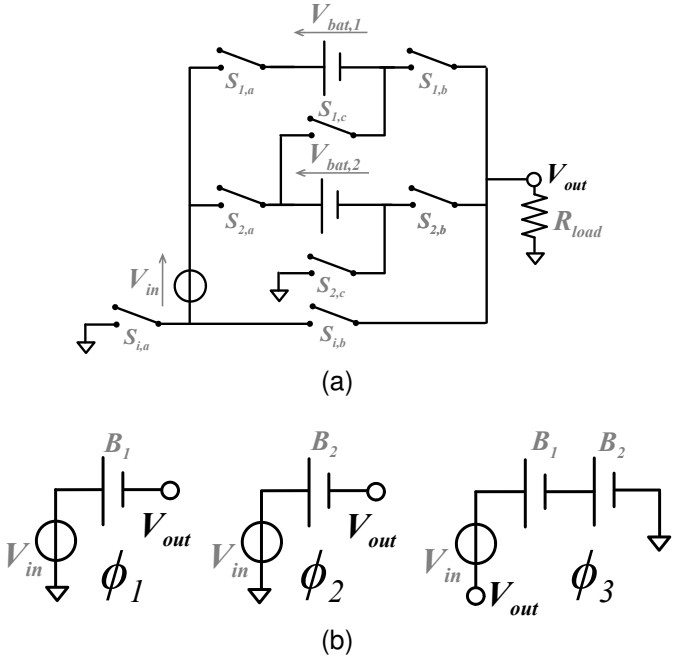

Fig. 9. 3:1 SBC topology: (a) electrical schematic and (b) operating phases

terminals. It can be observed that the maximum voltage across the switch terminals is $V_{in}/3$. This value represents a low power requirement for the switches. In comparison, in a 3:1 series-parallel SCC, certain switches would need to withstand a voltage of $2/3 \cdot V_{in}$ across their terminals when open while still conducting a current equal to I_{out} when closed.

B. Experimental Validation

The proposed 3:1 SBC configuration is implemented using both batteries, B1 and B2 (2V15H), which operate within the voltage range of 2 V to 2.8 V. With both batteries operating at 2 times the output voltage, the conversion range of the 3:1 SBC is suitable for input-to-output voltage ratios ranging from 3-to-1 up to 4.2-to-1. For the implementation, a battery voltage of 2.5 V is chosen, resulting in the 3:1 SBC converting an input voltage of 3.75 V to an output voltage of 1.25 V. Off-the-shelf CMOS analog switches (MAX4678) are used in the implementation, controlled by an external circuit that generates the three phases of equal duration. The equivalent output resistance can be calculated using Equation (2), which yields a value of 8.7 Ω. It is important to note that a significant contribution (31%) to this value comes from the internal resistance of the batteries, as discussed in Section III-B. This contribution is less prominent compared to the 2:1 SBC configuration but still larger than the contribution of the equivalent series resistance (ESR) in any SCC circuit.

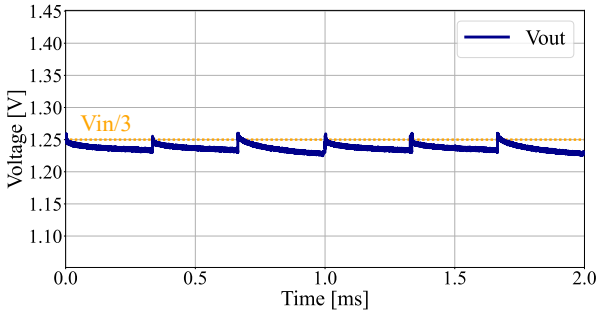

Fig. 10. 3:1 SBC output voltage waveform

The 3:1 SBC exhibits a settling time before reaching steady-state operation, during which both batteries (B1 and B2) demonstrate the self-adjustment behavior described in Section IV-D. Although the voltages of the two batteries were not exactly equal prior to the experiment (in open circuit), they both eventually reached a voltage of 2 times the output voltage required by the topology, with a minor voltage difference of 10 mV between them. Output voltage waveform of the 3:1 SBC is shown in Fig. 10.

Fig. 11 depicts the measured and calculated efficiency of the 3:1 SBC for various output currents,excluding control circuitry power consumption. Measured values are provided for two operating frequencies (100 Hz and 1 kHz) for both configurations. The calculated efficiency utilizes the previously determined frequency-independent equivalent output resistance. The average difference between the measured efficiency and the calculated efficiency is less than 1%. Similar to the 2:1 SBC configuration discussed in Section IV, the efficiency performance of the 3:1 SBC is relatively unaffected by frequency, within the limitations imposed by the range of ion mobility in the battery.

A high conduction efficiency (>90%) is achieved for an

output current exceeding 10 mA, even at a low switching frequency of 100 Hz, without the presence of any output capacitance. With this sustained high efficiency at 100 Hz, the 3:1 SBC achieves an output power of 15 mW, corresponding to a power density of 60 µW/mm^3 (considering only the volume occupied by the batteries). In comparison to the 2:1 SBC that utilizes a different battery type, the 3:1 configuration offers nearly six times lower power volume density. Both topologies provide a similar output voltage range, but the 3:1 SBC employs twice the number of batteries (with both connected in series during phase ϕ_3), and each battery has larger dimensions. Additionally, the 3:1 circuit introduces increased complexity and necessitates additional switches (8 compared to the 4 in the 2:1 SBC), further limiting the achievable power density.

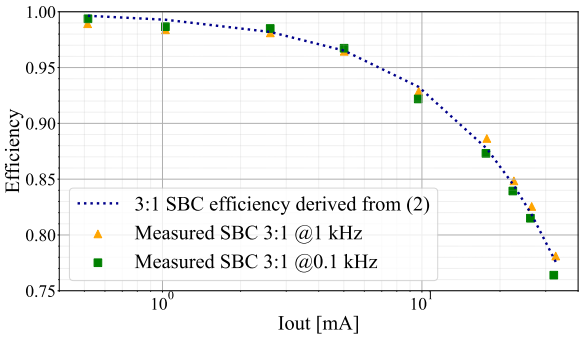

Fig. 11. Conversion efficiency of 3:1 SBC at different frequencies

Fig. 12 illustrates the relationship between the output voltage ripple and the output current for the 3:1 SBC at two distinct operating frequencies, namely 100 Hz and 1 kHz. Once again, these measurements were conducted without the presence of any output capacitance. The plot demonstrates that the output voltage ripple stays below 5% even at a low switching frequency of 100 Hz, with an output current of approximately 30 mA. Notably, this ripple level is lower than the corresponding value obtained with the 2:1 SBC under the same output current conditions.

In the case of the 3:1 SBC, the contribution of the batteries to the voltage ripple is advantageous due to their internal impedance, even when two batteries are connected in series during phase ϕ_3. This contribution can be equated to the term V_{IR} as depicted in Fig. 4b. Unlike the 2:1 SBC, which operates with only two phases, the 3:1 SBC employs three phases of equal duration. Consequently, the switching frequency of the 3:1 SBC is 1.5 times higher than that of the 2:1 SBC for the same cycle period. The higher switching frequency has a minor yet beneficial impact on the output voltage ripple at the same operating frequency.

VI. Discussion

Previous studies on ultra low-power DC-DC converters [14] [15] required operating at low frequencies in the Hz range to minimize switching losses, resulting in larger switched components (inductors or capacitors) to maintain acceptable output ripple. This paper presents batteries as an alternative solution

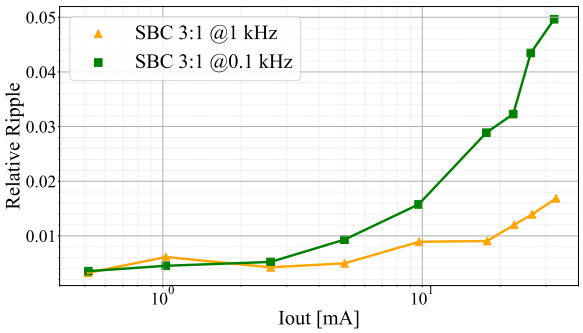

Fig. 12. 3:1 SBC low voltage output ripple in both frequencies (100 Hz and 1 kHz)

in low-power applications where conduction loss is not the primary concern. However, the usage of batteries is mainly limited for high-power levels by their relatively high equivalent series resistance (ESR) compared to capacitors and inductors, which is a result of physical laws. Consequently, batteries are more suitable for low current DC-DC converters. To further improve power capability, a co-optimization of circuit and battery design could be beneficial. Existing batteries derouted from their primary application of long-term energy storage have a dominant limitation of series resistance. However, the design of new batteries to obtain lower internal resistance while maintaining low DoD ($<<1\%$) could be envisioned in the future.

Despite a limited power-capability of the battery in comparison to existing SCC using flying capacitor, the SBC offers an undeniable advantage. Indeed, a key difference between these two architectures is that SCC experiences a natural tradeoff between its inherent charge-sharing losses and switching losses at low power levels [24]. Following equation gives the condition to meet in the case of 2:1 SCC:

$$\frac{1}{4C_{fly}f_{sw}}I_{out}^2 = f_{sw}Q_gV_{gs} \tag{4}$$

With f_{sw} the switching frequency, C_{fly} the flying capacitance, I_{out} the load current, Q_g the summed transistor gate charge and V_{gs} the transistor gate-source voltage swing. We deduce from (4) the optimum frequency to maximize efficiency:

$$f_{sw}^* = \frac{1}{\sqrt{4C_{fly}Q_gV_{gs}}}I_{out} \tag{5}$$

Hence SCC switching frequency at low output power level cannot be scaled down to any value but is limited by this tradeoff. To decrease f_{sw}^* or, equivalently, improve efficiency (at constant charge-sharing losses), the flying capacitance C_{fly} has to be increased, what degrades the power density of the converter. In contrast, SBC doesn't face this tradeoff, allowing its switching frequency to be reduced as much as needed to enhance efficiency at lower output power levels. This results in the existence of a critical-power operating point. Beyond this point, SCC outperforms SBC due to its lower equivalent series resistance (ESR). However, when operating at power levels

below this critical point, SBC exhibits superior efficiency due to its consistent output impedance across different frequencies.

An interesting and unexpected behavior observed in the SBC is its hybrid nature, exhibiting characteristics of both a battery and a capacitor. The DC biasing in the SBC is imposed by the DC-DC converter operation, similar to a capacitor, rather than solely relying on the battery itself. However, the SBC retains the desirable property of having its voltage nearly independent of the charge transferred during each cycle.

In order to gain a comprehensive understanding of the battery's lifetime under µ-cycles, a thorough investigation is required. The initial results obtained and previous research studies have highlighted a strong correlation between the depth of discharge (DoD) and the cycling endurance of batteries. By carefully managing the depth of discharge during micro-cycles, which is kept below parts per million (ppm) level, it is anticipated that the battery's cycling endurance can be significantly extended compared to the limited full charge/discharge cycles specified in battery datasheets. This presents encouraging prospects for the long-term operation of the DC-DC converter, as the battery's lifetime can be effectively prolonged by operating within the µ-cycle range. However, further research and analysis are necessary to delve deeper understanding into the battery's endurance under µ-cycles to ensure the sustained performance of the DC-DC converter over an extended period.

The temperature robustness aspect has not been addressed in detail within this paper. It is worth noting that batteries generally have a lower operating temperature range compared to capacitors, with upper limits rarely exceeding 80°C. This temperature limitation may pose some challenges for certain applications. However, in specific scenarios where low-power power management is required, such as in human devices, the slightly higher temperature range (around 37°C) could actually benefit the power capability demonstrated in this paper at room temperature (20-25°C). This is because the output impedance of the batteries decreases with temperature, leading to an improved power capability. Although the reduced energy capability at high temperatures may be a concern, it is important to highlight that the batteries in this setup are utilized within µ-cycles, where the amount of charge used (Q) is much smaller than the total energy storage capacity (Q_T) of the batteries. Therefore, the impact of reduced energy capability at higher temperatures is minimized. Further investigation and research are necessary to confirm these trends and thoroughly explore the temperature effects on the performance of the proposed topology.

The proposed SBC operates in open-loop, and future work requires exploration of closed-loop configurations to regulate the output voltage. Frequency modulation, a popular control solution in SCC [25], is not suitable for SBC, as the output impedance is largely frequency-independent. A two-stage control strategy could be explored: i) a coarse grain control implemented by changing the sequence (as a gearbox in SCC [26], [27]), and ii) a fine grain control using a LDO at the SBC output. One benefit of the SBC's low switching frequency operation is that it limits the LDO PSRR requirement, helping to reduce the quiescent current and thus maintain high power efficiency at light loads [28]. Another possible route is a hybrid version of SBC, as in SCC [29], [30], to allow duty-cycle control, or resonant-based [31].

The ultra-low switching frequency is also beneficial for lowering electromagnetic interference (EMI) experienced in SCC, further reducing the input and output EMI filtering requirements [32].

VII. Conclusion

In this paper, we have introduced the switched-battery converter (SBC) as a novel type of DC-DC converter specifically designed for ultra-low power applications in the milliampere and below range. The SBC utilizes batteries as flying passive components, enabling operation at extremely low frequencies in the hertz range to minimize switching losses. Unlike traditional battery management systems, the SBC employs batteries that experience µ-cycle variations, resulting in significantly different behavior compared to regular battery operation.

Compared to the more commonly used switched-capacitor converters (SCC), the SBC offers several advantages. Batteries in the SBC do not suffer from frequency-dependent output impedance in a first-order approximation, allowing for ultra-low switching frequencies and reduced losses at light loads. The paper presents two SBC topologies for step-down conversion, namely the 3:1 and 2:1 configurations, demonstrating the feasibility and effectiveness of the SBC approach.

The experimental results show that the SBC achieves high power efficiency, surpassing 90% for output currents greater than 10 mA, even at a low switching frequency of 100 Hz. With a compact volume in the range of tens of cubic millimeters, the SBC is well-suited for low-output-power DC-DC converters up to several tens of milliwatts. Furthermore, the unique charging and discharging characteristics of the battery in the SBC result in significantly extended battery lifetime, with reported lifetimes of up to 10^9 cycles without degradation.

The paper also demonstrates the versatility of the SBC by exploring its operation with different battery chemistries and proposes a multiple batteries SBC configuration (3:1) to further reduce the dependency between output and battery voltages. These initial findings indicate that the SBC could be a promising option for certain low-power DC-DC converter applications. With advancements in dense integration of batteries in solid-state materials, the scalability of footprint and the use of multiple batteries can further enhance the potential of the SBC.

References

[1] J. Deng, J.-L. Nagel, L. Zahnd, M. Pons, D. Ruffieux, C. Arm, P. Persechini, and S. Emery, "Energy-autonomous mcu operating in sub-vt regime with tightly-integrated energy-harvester : A soc for iot smart nodes containing a mcu with minimum-energy point of 2.9pj/cycle and a harvester with output power range from sub-μw to 4.32mw," in *2019 IEEE/ACM International Symposium on Low Power Electronics and Design (ISLPED)*, 2019, pp. 1–4.

[2] G. Chowdary and S. Chatterjee, "A 300-nw sensitive, 50-na dc-dc converter for energy harvesting applications," *IEEE Transactions on Circuits and Systems I: Regular Papers*, vol. 62, no. 11, pp. 2674–2684, 2015.

[3] M. Krstic, S. Eren, and P. Jain, "Analysis and design of multiphase, reconfigurable switched-capacitor converters," *IEEE Journal of Emerging and Selected Topics in Power Electronics*, vol. 8, no. 4, pp. 4046–4059, 2020.

[4] Y. Lu, J. Jiang, and W.-H. Ki, "Design considerations of distributed and centralized switched-capacitor converters for power supply on-chip," *IEEE Journal of Emerging and Selected Topics in Power Electronics*, vol. 6, no. 2, pp. 515–525, 2018.

[5] M. D. Seeman, V. W. Ng, H.-P. Le, M. John, E. Alon, and S. R. Sanders, "A comparative analysis of Switched-Capacitor and inductor-based DC-DC conversion technologies," in *2010 IEEE 12th Workshop on Control and Modeling for Power Electronics (COMPEL)*, Jun. 2010, pp. 1–7, iSSN: 1093-5142.

[6] A. Kushnerov, "Multiphase fibonacci switched capacitor converters," *IEEE Journal of Emerging and Selected Topics in Power Electronics*, vol. 2, no. 3, pp. 460–465, 2014.

[7] E. Perez, C. A. Berlitz, Y. Moursy, B. Allard, S. Oukassi, and G. Pillonnet, "Ultra-low frequency dc-dc converters using switched batteries," in *2022 IEEE Energy Conversion Congress and Exposition (ECCE)*, 2022.

[8] S. Moury and J. Lam, "A soft-switched power module with integrated battery interface for photovoltaic-battery power architecture," *IEEE Journal of Emerging and Selected Topics in Power Electronics*, vol. 8, no. 3, pp. 3090–3110, 2020.

[9] Y. Ye and K. W. E. Cheng, "Modeling and analysis of series–parallel switched-capacitor voltage equalizer for battery/supercapacitor strings," *IEEE Journal of Emerging and Selected Topics in Power Electronics*, vol. 3, no. 4, pp. 977–983, 2015.

[10] W. Han, T. Wik, A. Kersten, G. Dong, and C. Zou, "Next-generation battery management systems: Dynamic reconfiguration," *IEEE Industrial Electronics Magazine*, vol. 14, no. 4, pp. 20–31, 2020.

[11] S. K. Pradhan and B. Chakraborty, "Battery management strategies: An essential review for battery state of health monitoring techniques," *Journal of Energy Storage*, vol. 51, p. 104427, 2022. [Online]. Available: https://www.sciencedirect.com/science/article/pii/S2352152X22004509

[12] . Murata Manufacturing Co. Ltd., "ECASD40J107M015K00." [Online]. Available: https://www.murata.com/en-eu/products/productdetail?partno=ECASD40J107M015K00

[13] . Murata Manufacturing Co., "LQH44NN471K03." [Online]. Available: https://www.murata.com/en-eu/products/productdetail?partno=LQH44NN471K03%23

[14] A. Paidimarri and A. P. Chandrakasan, "10.8 a buck converter with 240pw quiescent power, 922017 *IEEE International Solid-State Circuits Conference (ISSCC)*, 2017, pp. 192–193.

[15] X. Liu, S. Li, and B. H. Calhoun, "An 802pw 93with 5.5×106 dynamic range featuring fast dvfs and asynchronous load-transient control," in *ESSCIRC 2021 - IEEE 47th European Solid State Circuits Conference (ESSCIRC)*, 2021, pp. 347–350.

[16] S. Oukassi, A. Bazin, C. Secouard, I. Chevalier, S. Poncet, S. Poulet, J.-M. Boissel, F. Geffraye, J. Brun, and R. Salot, "Millimeter scale thin film batteries for integrated high energy density storage," in *2019 IEEE International Electron Devices Meeting (IEDM)*, Dec. 2019, pp. 26.1.1–26.1.4.

[17] J. Celè, S. Franger, Y. Lamy, and S. Oukassi, "Minimal architecture lithium batteries: Toward high energy density storage solutions," *Small (Weinheim an der Bergstrasse, Germany)*, p. e2207657, 2023.

[18] M. Alahmad, H. Hess, M. Mojarradi, W. West, and J. Whitacre, "Battery switch array system with application for jpl's rechargeable micro-scale batteries," *Journal of Power Sources*, vol. 177, no. 2, pp. 566–578, 2008. [Online]. Available: https://www.sciencedirect.com/science/article/pii/S0378775307025293

[19] J. W. Evans, B. Kim, S. Ono, A. C. Arias, and P. K. Wright, "Multicycle testing of commercial coin cells for buffering of harvested energy for the iot," *IEEE Internet of Things Journal*, vol. 8, no. 12, pp. 10 047–10 051, 2021.

[20] M. D. Seeman and S. R. Sanders, "Analysis and optimization of switched-capacitor dc–dc converters," *IEEE Transactions on Power Electronics*, vol. 23, no. 2, pp. 841–851, 2008.

[21] M. Krstic, S. Eren, and P. Jain, "Curvature-based average modeling of switched-capacitor converters," *IEEE Journal of Emerging and Selected Topics in Power Electronics*, vol. 9, no. 5, pp. 5929–5940, 2021.

[22] T. V. Breussegem and M. Steyaert, "A 82integrated capacitive voltage doubler," in *2009 Symposium on VLSI Circuits*, 2009, pp. 198–199.

[23] J. W. Evans, B. Kim, S. Ono, A. C. Arias, and P. K. Wright, "Multicycle Testing of Commercial Coin Cells for Buffering of Harvested Energy for the IoT," *IEEE Internet of Things Journal*, vol. 8, no. 12, pp. 10 047–10 051, Jun. 2021.

[24] E. Perez, Y. Moursy, S. Oukassi, and G. Pillonnet, "Silicon capacitors opportunities for switched capacitor converter," in *2022 IEEE 23rd Workshop on Control and Modeling for Power Electronics (COMPEL)*, 2022.

[25] T. Souvignet, B. Allard, and S. Trochut, "A fully integrated switched-capacitor regulator with frequency modulation control in 28-nm fdsoi," *IEEE Transactions on Power Electronics*, vol. 31, no. 7, pp. 4984–4994, 2016.

[26] G. Pillonnet, A. Andrieu, and E. Alon, "Dual-input switched capacitor converter suitable for wide voltage gain range," *IEEE Journal on Emerging and Selected Topics in Circuits and Systems*, vol. 5, no. 3, pp. 413–420, Feb. 2015.

[27] M. Krstic, S. Eren, and P. Jain, "Analysis and design of multiphase, reconfigurable switched-capacitor converters," *IEEE Journal of Emerging and Selected Topics in Power Electronics*, vol. 8, no. 4, pp. 4046–4059, 2020.

[28] A. Quelen, F. Badets, and G. Pillonnet, "A sub-100nw power supply unit embedding untrimmed timing and voltage references for duty-cycled μw-range load in fdsoi 28nm," in *43rd IEEE Eur. Solid State Circuits Conf. (ESSCIRC)*, Sept. 2017, pp. 279–282.

[29] Y. Lei and R. Pilawa-Podgurski, "Soft-charging operation of switched-capacitor dc-dc converters with an inductive load," in *Proc. IEEE Applied Power Electronics Conference and Exposition*, 2014, p. 2112-2119.

[30] S. R. Pasternak, M. H. Kiani, J. S. Rentmeister, and J. T. Stauth, "Modeling and performance limits of switched-capacitor dc–dc converters capable of resonant operation with a single inductor," *IEEE Journal of Emerging and Selected Topics in Power Electronics*, vol. 5, no. 4, pp. 1746–1760, 2017.

[31] E. Abramov, A. Cervera, and M. M. Peretz, "Optimal design of a voltage regulator based on gyrator switched-resonator converter ic," *IEEE Journal of Emerging and Selected Topics in Power Electronics*, vol. 6, no. 2, pp. 549–562, 2018.

[32] J. Zhou and W. Dehaene, "Fully integrated cmos eme-suppressing current regulator for automotive electronics," *IEEE Transactions on Circuits and Systems I: Regular Papers*, vol. 59, no. 2, pp. 266–275, 2012.

Carlos Augusto Berlitz was born in Campo Bom, Brazil, in 1991. He received the electrical engineering degree from Universidade Federal do Rio Grande do Sul, Porto Alegre, Brazil, in 2017, and the M. Sc. degree in electronics, electrical energy and automation from University of Grenoble Alps, Grenoble, France, in 2019 . He is pursuing a Ph.D. degree from Ampère Laboratory, National Institute of Applied Sciences of Lyon, Villeurbanne, France in partnership with CEA-Leti, Grenoble, France.

Emeric Perez (M'21) was born in France in 1998. He received his Master's degree in Electrical Engineering from Grenoble Institute of Technology Ense3, France, with a specialization in power electronics. Currently pursuing towards a Ph.D degree at CEA-Leti and Grenoble Alpes University, France, his main research interests includes power management, switched-capacitor converters and micro-batteries applied to dc-dc conversion. He is also involved in teaching activities of power electronics at Master's level in its former university.

Sami Oukassi was born in Bizerte, Tunisia, in 1980. He received his Master's degree in Materials science from INP Grenoble, France, in 2004, and a PhD from Université Paris Est, France in 2008. Since 2008, he joined CEA Leti, Grenoble, France. He is now head of laboratory for RF and energy storage devices. His research focuses on solid state ionics, in particular applied ionics in devices for energy micro-storage (batteries, supercapacitors), optoelectronics (chromogenics), and data storage (synaptic transistors). He is co-author of 20 publications and 50 patents.

Bruno Allard (SM'02) received the M.Sc. and Ph.D. degrees in microelectronics engineering from INSA Lyon, France, in 1989 and 1992, respectively. He is a Full Professor in Electrical Engineering at INSA in Lyon. He is the past Head Manager of Ampere-lab (staff of 80 researchers and 120 PhD students). He has led numerous industrial and academic projects. His research interests include the integration of power systems, either hybrid or monolithic, for fine voltage conversion and/or energy harvesting, low-power electronic system design and low-power monolithic converter design. He is active in the fields covered by the PELS workshop PwrSoC, that bridges the gap between power electronics (PELS), integrated systems (CAS), industrial electronics (IES) and energy harvesting (MTT). He is the author or coauthor of +130 papers in Transactions and Journals and +300 international conference articles. He has been a member of IEEE PELS AdCom and currently member-at-large in the IEEE IES AdCom.

Gaël Pillonnet (M'05, SM'16) was born in Lyon, France, in 1981. He received his Master's degree in Electrical Engineering from CPE Lyon, France, in 2004, a PhD and habilitation degrees from INSA Lyon, France in 2007 and 2016, respectively. Following an early experience as analog designer in STMicroelectronics in 2008, he joined the University of Lyon as associate Professor. During the 2011-12 academic year, he held a visiting researcher position at the University of California at Berkeley. Since 2013, he is in CEA-Léti, Grenoble, France, involved in developing various projects in design technology co-optimization. During the 2022-2023 academic year, he joins energy-efficient microsystems group at UCSD as a visiting researcher. He is now the scientific advisor for the Silicon component division in CEA-Léti. His research focuses on power-conversion oriented circuits such as DC-DC converters, audio amplifiers, adiabatic logics, electromechanical transducers, harvesting electrical interfaces. He is also involved in various device/circuit design enablement for RRAM, Si-qubit, solid-state energy storage and MEMS sensors.